Nonlinear optical response of wave packets on quantized potential energy surfaces

Kunio Ishida and Fumihiko Aiga
Corporate Research and Development Center, Toshiba Corporation
1 Komukaitoshiba-cho, Saiwai-ku, Kawasaki 212-8582, Japan
and
Kazuhiko Misawa
Department of Applied Physics,
Tokyo University of Agriculture and Technology
2-24-16 Naka-cho, Koganei, Tokyo 184-8588, Japan

Abstract

We calculated the dynamics of nuclear wave packets in coupled electron-vibration systems and their nonlinear optical responses. We found that the quantized nature of the vibrational modes is observed in pump-probe spectra particularly in weakly interacting electron-vibration systems such as cyanine dye molecules. Calculated results based on a harmonic potential model and molecular orbital calculations are compared with experimental results, and we also found that the materials parameters regarding with the geometrical structure of potential energy surfaces are directly determined by accurate measurement of time-resolved spectra.

1 Introduction

Optical control of quantum-mechanical states has attracted attention of many authors[1]. In particular, recent progress in laser technology has made it possible to synthesize desired optical pulses, and they are expected to be a tool to control physical properties of various materials, *e.g.*, luminescence intensity, lifetime of excited states, or chemical reaction rate.

We, however, have not found effective methods for coherent control of those properties, since it is impossible to design appropriate optical processes without the knowledge of the structure

of the electronic states and/or the potential energy surfaces (PESs) of materials. Thus, it is important to determine the values of the material parameters regarding with the ground-state and/or excited-state PESs to realize coherent control of above-mentioned physical properties. As a first step toward this approach, we study methods to trace the motion of wave packets on each PES after photoexcitation in order to understand the structure of PESs.

Experimental studies on wave packet dynamics have been performed with ultrashort laser pulses since the pioneering work by Zewail *et al.*[2], and previous studies on molecules in solution give a clue to understand the motion of wave packets created by optical pulses[3, 4, 5, 6]. Although the nonlinear response of wave packets on PESs has been understood by means of the motion of a "classical point" on PESs, our recent experiments on cyanine dye molecules have shown that the wave packet dynamics in those molecules is understood only by taking into account the quantum nature of the vibrational modes of the molecules[7]. According to our preliminary calculations[7], this particular feature is obtained when the interaction between electrons and the vibrational modes is weak. To be more precise, the quantum nature of vibrational modes becomes prominent when the average number of vibrational quanta contained in each wave packet is ~ 1, which shows that the wave packet motion is restricted in the vicinity of the bottom of the PESs. In this case, the relaxation energy of the Franck-Condon state is comparable to the energy of vibrational quanta $\hbar\omega$.

In this paper we calculate the dynamics and the nonlinear optical response of wave packets on excited-state PES when quantization of vibration modes plays an important role, *i.e.*, in weakly coupled electron-vibration systems. In this particular case, we found that the impulse approximation is effective to analyze the experimental data. We also show that accurately measured pump-probe signals help us determine the values of the material parameters regarding with the structure of PESs, which are, as mentioned before, important to design the coherent control methods of wave packets by laser pulses.

The paper is organized as follows: in Section 2 we introduce the model and its basic properties. We show the calculated results of the pump-probe signal including the molecular orbital calculation for cyanine dye molecules in Section 3. Section 4 is devoted to discussion and conclusions.

2 Model

In order to describe the dynamics of wave packets in typical organic molecules, we take into account relevant two electronic states which correspond to the ground and the excited states and interact with multiple vibrational modes. Thus, we employ the simplest model suitable for the present purpose, *i.e.*, a two-level model on potential surfaces with M modes described by

the following Hamiltonian:

$$\mathcal{H} = \sum_{j=1}^{M} \left\{ \frac{p_j^2}{2} + \frac{\omega_j^2}{2} q_j^2 + \left(\hbar\omega_j s_j^2 + \sqrt{2\hbar\omega_j^3} s_j q_j + \frac{t_j \omega_j^2}{2} q_j^2 \right) | \uparrow\rangle\rangle\langle\langle\uparrow | \right\} + \hbar\varepsilon | \uparrow\rangle\rangle\langle\langle\uparrow |. \tag{1}$$

In Eq. (1) $| \uparrow\rangle\rangle$ denotes the excited electronic state of a single molecule, and its ground electronic state is $| \downarrow\rangle\rangle$. p_j and q_j are the normalized momentum and the coordinate of the vibration modes of the molecule, and s_j is the dimensionless coupling constant between an electron and the j-th vibrational mode.

Since, in weakly coupled electron-vibration systems, the wave packet motion is restricted only in the vicinity of the bottom of PES as mentioned before, the parabolic approximation is appropriate in the present study. In particular, a Gaussian wave packet which is generated by the vertical transition by optical field does not distort while it moves on parabolic PESs. This property appears to be quite useful, as the optical response within the impulse approximation is obtained analytically as shown in the next section.

In the rest of the paper, we assume that the vibrational frequencies on both PESs are the same, *i.e.*, we take $t_j = 0$, which is appropriate for cyanine dye molecules as shown in the next section. The details of the quantization of the Hamiltonian (1) is also described in the Appendix A, and we show in this section only the eigenvalues and eigenstates of Hamiltonian (1) corresponding to the ground-state PES and the excited-state PES for $t_j = 0$:

1. ground-state PES

$$E^{\downarrow}_{n_1,n_2,\ldots,n_M} = \hbar \sum_{j=1}^{M} n_j \omega_j \tag{2}$$

$$|n_1, n_2, ..., n_M \downarrow\rangle = |n_1, n_2, ..., n_M\rangle \otimes | \downarrow\rangle\rangle. \tag{3}$$

2. excited-state PES

$$E^{\uparrow}_{n_1,n_2,\ldots,n_M} = \hbar \left(\sum_{j=1}^{M} n_j \omega_j + \varepsilon \right) \tag{4}$$

$$|n_1, n_2, ..., n_M \uparrow\rangle = \prod_{j=1}^{M} e^{-s_j (a_j^\dagger - a_j)} |n_1, n_2, ..., n_M\rangle \otimes | \uparrow\rangle\rangle, \tag{5}$$

where the boson number states (Fock states) are defined by

$$|n_1, n_2, ..., n_M\rangle = \bigotimes_{j=1}^{M} \frac{(a_j^\dagger)^{n_j}}{\sqrt{n!}}|0\rangle. \tag{6}$$

3 Calculated results

3.1 Pump-probe signals of wave packets on harmonic potential surface

When we consider that the temporal width of both the pump and the probe pulses are small compared with the period of vibration modes $2\pi/\omega_j$, we apply the impulse approximation to calculate the probe signal[8] as

$$A(\Omega; T) \propto \mathrm{Im}\left[\int_0^\infty P(T,t)e^{i\Omega(t-T)}dt\right], \tag{7}$$

where the time-dependent polarization induced by the probe pulse $P(T,t)$ is given by

$$P(T,t) = \frac{i}{\hbar}\langle\Phi(T)|[V(t-T), V]|\Phi(T)\rangle\theta(t-T). \tag{8}$$

Ω and T denote the frequency and the delay of the probe pulse, respectively, and $\theta(t)$ is the step function.

The wavefunction $|\Phi(T)\rangle$ is the Franck-Condon state multiplied by the time-evolution operator with regard to $\mathcal{H}$ and is described by

$$\begin{aligned} |\Phi(T)\rangle &= e^{-\frac{i\mathcal{H}T}{\hbar}}|s_1, s_2, ..., s_M; \uparrow\rangle \\ &= e^{-i\varepsilon T}|s_1 e^{-i\omega_1 T}, s_2 e^{-i\omega_2 T}, ...s_M e^{-i\omega_M T}; \uparrow\rangle, \end{aligned} \tag{9}$$

where $|\alpha_1, \alpha_2, ...\alpha_M; \uparrow\rangle$ is a Gaussian wave packet on the excited-state PES, *i.e.*, a coherent state of the vibration modes defined by

$$\begin{aligned} &|\alpha_1, \alpha_2, ..., \alpha_M; \uparrow\rangle \\ = &\sum_{n_1, n_2, ..n_M=0}^{\infty} \prod_{j=1}^{M} \frac{e^{-\frac{|\alpha_j|^2}{2}}\alpha_j^{n_j}}{\sqrt{n_j!}}|n_1, n_2, ..., n_M \uparrow\rangle. \end{aligned} \tag{10}$$

The polarization operator is given by $V = |\uparrow\rangle\rangle\langle\langle\downarrow| + |\downarrow\rangle\rangle\langle\langle\uparrow|$ and its time-dependent form $V(t)$ is

$$V(t) = e^{\frac{i\mathcal{H}t}{\hbar}} V e^{-\frac{i\mathcal{H}t}{\hbar}}, \tag{11}$$

in the interaction representation.

After algebraic calculations, $P(T,t)$ is obtained as

$$P(T,t) = \mathrm{Im}\left(\frac{e^{i\varepsilon(t-T)}}{\hbar}\prod_{j=1}^{M}\bar{p}_j(T,t)\right)\theta(t-T), \tag{12}$$

where

$$\begin{aligned}\bar{p}_j(T,t) &= \exp\{-s_j^2(1-e^{i\omega_j t}-e^{-i\omega_j T}+e^{-i\omega_j t}+e^{i\omega_j T}-e^{-i\omega_j(t-T)})\} &(13)\\ &= e^{-s_j^2(1+2i\sin\omega T)}\sum_{n=0}^{\infty}\frac{s_j^{2n}}{n!}\sum_{l+m\le n}\frac{(-)^m}{l!m!(n-l-m)!}e^{-i\omega_j(n-2l)t}e^{-i\omega_j(n-l-m)T}. &(14)\end{aligned}$$

Combining Eqs. (7), (12), and (14), we found that finite probe signal is obtained only when the resonance condition

$$\Omega = \varepsilon + \sum_{j=1}^{M} k_j\omega_j \quad (k_j = 0, \pm1, \pm2, ..), \tag{15}$$

is satisfied.

For $M = 1$, $P(t,T)$ has a far simpler form and $A(\Omega;T)$ is analytically obtained for arbitrary value of Ω and T. When we consider the case for $M = 1$ the indices of the parameters are omitted for brevity in the rest of the paper. The Fourier transformation of $P(t,T)$ is performed in a straightforward manner and $A(\Omega;T)$ is given by

$$\begin{aligned}A(\Omega;T) \propto \frac{1}{\hbar}\mathrm{Im}\Bigg[&e^{-s^2(1-2i\sin\omega T)}\sum_{n=-[\varepsilon\omega]}^{\infty}\frac{e^{-in\omega T}}{(1-e^{-i\omega T})^{n/2}}J_n\left(2s^2\sqrt{1-e^{-i\omega T}}\right)\delta(\Omega-\varepsilon-n\omega)\\ +\ &e^{-s^2(1+2i\sin\omega T)}\sum_{n=-\infty}^{-[\varepsilon\omega]-1}\frac{e^{in\omega T}}{(1-e^{i\omega T})^{n/2}}J_n\left(2s^2\sqrt{1-e^{i\omega T}}\right)\delta(\Omega+\varepsilon+n\omega)\Bigg],\end{aligned} \tag{16}$$

where $J_n(z)$ is the Bessel function of the first kind and $[a]$ denotes the largest integer which does not exceed the value of a. When $s^2 \gg 1$, vibration eigenstates are densely distributed between the Franck-Condon state and the bottom of the excited-state PES, which means that

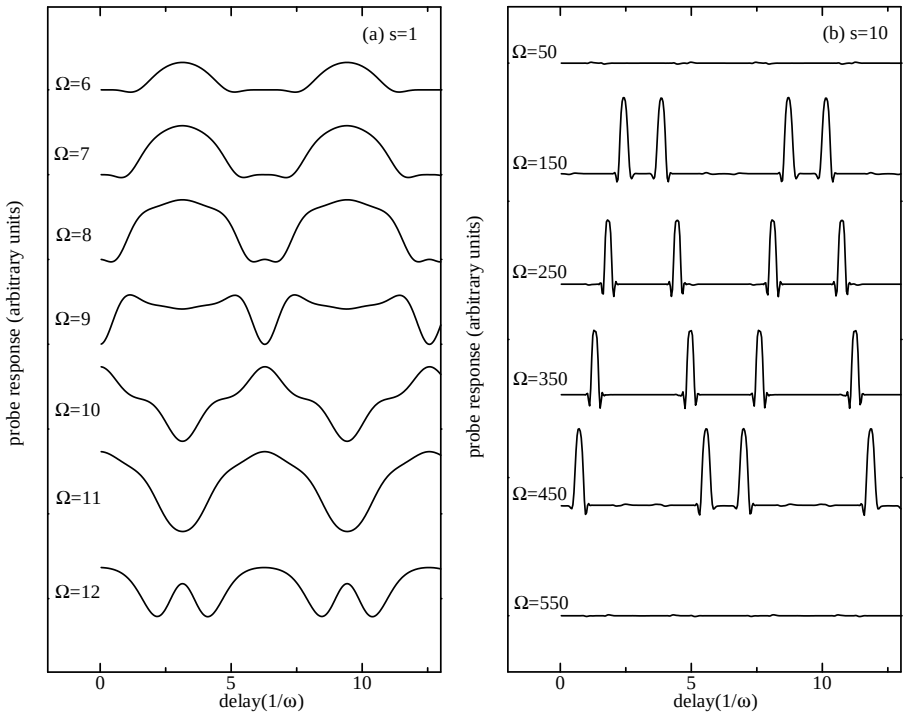

Figure 1: Probe response for $M = 1$ and (a) $s = 1, \varepsilon = 10$, (b) $s = 10, \varepsilon = 100$. Ω denotes the probe frequency in units of $\hbar\omega$.

the classical picture based on continuous PESs is recovered. For example, $A(\Omega; 2n\pi/\omega)$ ($n = 0, 1, 2, 3...$) is obtained as

$$A(\Omega; 2n\pi/\omega) \propto \frac{1}{\hbar} \sum_{j=0}^{\infty} \frac{e^{-s^2} s^{2j}}{j!} \delta(\Omega - \varepsilon - j\omega). \tag{17}$$

The coefficients on each δ-function in Eq. (17) show that the probe response as a function of probe frequency is given by the Poisson distribution which approaches the normal distribution in the limit of $s \to \infty$.

We numerically calculated $A(\Omega; T)$ for arbitrary values of Ω or T, and Figs. 1-(a) and (b) show the probe response as a function of T for several values of Ω for $s = 1$ and $s = 10$, respectively. When $s = 10$, the temporal behavior of the probe response is understood by means of a classical PES, *i.e.*, finite reponse to the probe pulse is observed only when the center of the wave packet passes the point on the PES at which the probe pulse resonates to the transition between $|\downarrow\rangle$ and $|\uparrow\rangle$. However, when $s = 1$, the quantum nature of the vibration

mode appears to be important and the shape of the probe spectra as a function of pump-probe delay T apparently differs from that obtained from classical PESs, *i.e.*, the probe response is finite even when the center of the wave packet is not on the resonating point of the PES to the probe pulse. In other words, the probe signal is temporally broadened due to the finite spatial width of the quantum-mechanical wave packet.

Reflecting the motion of the wave packet, the probe signal shows a oscillatory behavior as a function of T. In the classical limit the peaks of the oscillation in the spectra gradually move as the probe frequency is changed, whilst the peaks and the valleys in the spectra suddenly interchanges with each other as the change of the probe frequency in the quantum-mechanical regime. Thus the time-resolved spectra translationally move along the temporal axis as if their phase shifts by π. As Eq. (14) shows, however, the phase of the oscillation as a function of T does not alter, and thus the peak shift in the spectra cannot be discussed in terms of the phase of the oscillation. Hence, we stress that time-dependent shift of the phase in each Fourier component which is often taken into account in experimental studies is not necessary to analyze the time-resolved spectra to discuss the wave packet motion.

The quantum nature of the PESs is also shown in observing the "turning points" of the wave packet motion. When probe frequency is varied, we observe spectral structure which shows the turning points and they help us determine the values of material parameters[7]. Since, however, both the average and the variance of the number of vibrational quanta in a Gaussian wave packet $|s\uparrow\rangle$ are s^2, the probe response of wave packets is obtained for higher/lower probe frequencies than those at the classical turning points. As a result, the spectra become blurred as shown in experiments[7]. However, the peaks of the spectra still gives the turning points in classical sense, and therefore we expect that accurate measurement of time-resolved spectra is still an effective tool to obtain the values of materials parameters.

It has been pointed out that the probe signals include the optical response of wave packets on the ground-state PES as well as those on the excited-state PES[4]. Since, as shown in Eq. (7), the impulse approximation takes into account the signals only from the excited-state wave packets, it is necessary to consider the validity of the impulse approximation for the probe pulses with finite width.

Using the standard third-order perturbation theory[8], we found that the contribution of ground-state wave packets to the probe response can be estimated by the transition probability between the ground and excited PESs,

$$r^j_{n_1 n_2 \ldots n_M} = \prod_{j=1}^{M} \exp\{-2s_j^2(1-\cos\omega_j\tau)\}\frac{\{2s_j^2(1-\cos\omega_j\tau)\}^{n_j}}{n_j!}, \tag{18}$$

where τ denotes the temporal width of the pump pulse. The detail of the calculation to derive Eq. (18) is presented in Appendix B.

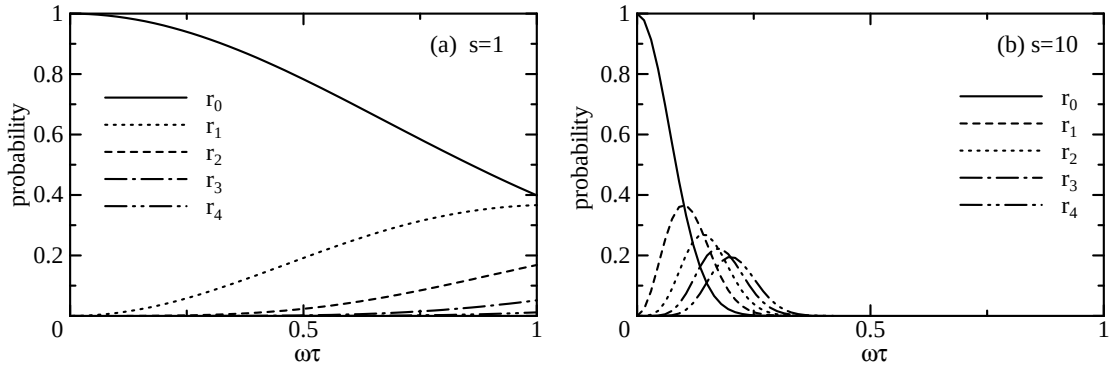

Figure 2: Transition probability r_n $(n = 0, 1, 2, 3, 4)$ for $M = 1$ and (a)$s = 1$, (b)$s = 10$.

Figure 2 show $r_n (n = 0, 1, 2, 3, 4)$ for $s = 1$ and $s = 10$ for $M = 1$. For $s = 1$, r_n for $n \neq 0$ is small compared with r_0 for $\omega\tau < 0.5$, which corresponds to the case where the pump pulse is shorter than the tenth of the vibrational period. For this short pulse, the ground-state wave packets generated by the pump pulse are dominated by $|0\downarrow\rangle$ which does not contribute to the temporal oscillation of the probe spectra, and hence only the motion of excited-state wave packets is reflected on the time-resolved spectra.

On the other hand, for $s = 10$, r_n for $n \neq 0$ is comparable to r_0 and hence the ground-state wave packets consist of multiple vibrational states. In this case, the time-resolved spectra contain oscillatory structure due to the motion of ground-state wave packets as well as that of the excited-state wave packets, and the impulse approximation fails.

Hence, we found that the validity of the impulse approximation is estimated by calculating the values of r_n. Comparing r_0 with r_1, we found that the impulse approximation works when $p_c = r_1/r_0 = 2s^2(1 - \cos\omega\tau)$ or, in general, all of the corresponding factors p_c^j for j-th mode are sufficiently small. In particular, for weakly coupled electron-vibration systems such as dye molecules $(s \leq 1)$, the probe signals given by the wave packets on the ground-state PES are independent of the delay T for short probe pulses used in experiments, and thus the present calculation is valid to discuss the motion of the excited-state wave packets.

3.2 Pump-probe response of cyanine dye molecules

3.2.1 Molecular Orbital Calculations

Before we apply the present theory to the optical properties of DTTCI (diethylthiatricarbocyanine iodide) measured in our previous study[7], we calculate the electronic state of DTTCI by the molecular orbital calculations. DTTCI is dissociated into $C_{25}H_{25}N_2S_2^+$ and I^- in the ethanol

solution. Therefore, we consider DTTC$^+$($C_{25}H_{25}N_2S_2^+$) as a model molecule, where the solvent effect is not considered. The optimized geometry for the singlet ground state of DTTC$^+$ was obtained in the restricted Hartree-Fock (RHF) approximation, and the vibrational frequency analysis was performed. The optimized geometry for the first singlet excited state was obtained in the singly excited configuration interaction (CIS) approximation, and the vibrational frequency analysis was performed. The basis set employed in this work was 6-31G(d)[9], and all calculations were performed with the Gaussian 98 program package[9].

The probability amplitudes for the highest occupied molecular orbital (HOMO) and the lowest unoccupied molecular orbital (LUMO) of DTTC$^+$ are given in Fig. 3. The character of

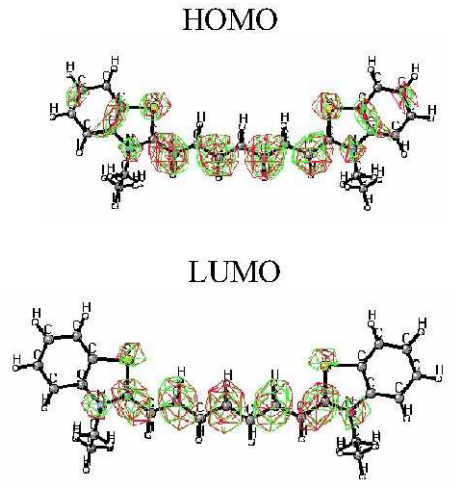

Figure 3: The probability amplitudes for HOMO and LUMO of DTTC$^+$.

the first excited state in the CIS calculation is the excitation from HOMO to LUMO. The large oscillator strength for this excitation, 2.94 in the CIS calculation, indicates that DTTCI is the efficient dye molecule.

Schematic representation of the potential energy surfaces for the ground ($E_g(\mathbf{R})$) and the first excited states ($E_x(\mathbf{R})$) of DTTC$^+$ is illustrated in Fig. 4. The minimum energy configuration for the ground state is shown as **A**, and that for the first excited state is shown as **B**. The difference of the configuration between **A** and **B** is quite small, and the energy difference $E_x(\mathbf{A}) - E_x(\mathbf{B})$ is so small as 52.5 meV. The difference between the vibrational frequency for the first excited state and that for the ground state is also quite small. Therefore, the weak coupling model can be applied to this problem, and the vibrational modes for the first excited state can be considered to be the same as those for the ground state.

In the Franck-Condon picture, absorbing the pump light, the DTTC$^+$ molecule is vertically excited from the ground state to the first excited state, and the DTTC$^+$ molecule is placed

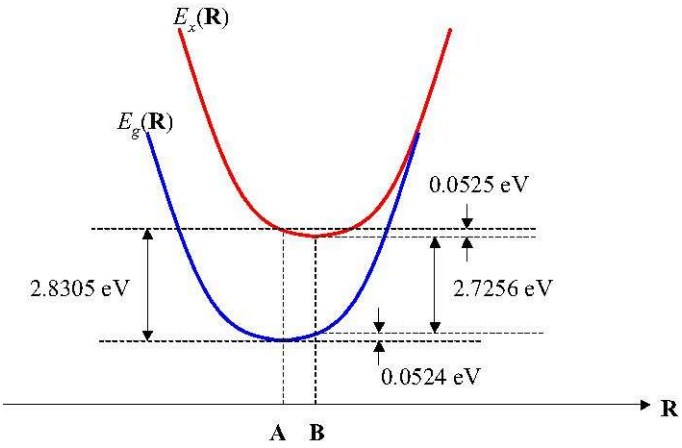

Figure 4: Schematic representation of the potential energy surfaces for the ground and the first excited states of $DTTC^+$.

on the configuration **A** on the potential energy surface of the first excited state ($E_x(\mathbf{A})$). In order to investigate the time-dependent nuclear dynamics of $DTTC^+$ molecule after the excitation, molecular dynamics (MD) calculation is necessary. Considering the nucleus as classical particles, the MD of $DTTC^+$ can be described by the Newtonian equation of motion with the potential ($E_x(\mathbf{R})$). Although we have not performed the full MD calculation, we have calculated the force at ($E_x(\mathbf{A})$),

$$\mathbf{F} = \left.\frac{\partial E_x(\mathbf{R})}{\partial \mathbf{R}}\right|_{\mathbf{R}=\mathbf{A}}, \tag{19}$$

as the measure of the initial dynamics. The vector **F** has 162 components corresponding to the x, y, and z directions of each atom. Then, the scalar product of **F** with each unit displacement vector $\mathbf{u}_i (i = 1 \sim 156)$ corresponding to each harmonic vibration on ($E_x(\mathbf{R})$) has been calculated. The vector $\mathbf{u}_i$ has 162 components as well.

The vibrational frequency modes, having larger absolute value for the scalar product with **F**, are given in Table 1, where **F** is normalized. The mode 45 has the largest absolute value for the scalar product. Considering the beat of our experiment has the period of $\sim$ 230 fsec, the frequencies for mode 15 is close to the experimental frequency. For further verification of the experiment, we have to perform the MD calculation .

3.2.2 Pump-probe spectra of DTTCI

To compare with the experimentally observed pump-probe spectra[7], we calculated the probe response based on Eq. (12) for $M = 2$. The values of the parameters of the vibrational

mode	frequency(cm^{-1})	$\mathbf{F}\cdot\ \mathbf{u}_i$
1	15.0427	0.06
8	86.5312	-0.06
15	191.0350	-0.07
17	219.8474	-0.06
22	292.0076	-0.12
31	443.1244	-0.07
37	550.7053	-0.06
39	574.0371	0.09
45	645.1332	-0.19
50	784.4855	0.06
51	792.6894	0.09
52	800.6848	0.07
53	800.7149	0.10
84	1232.1675	-0.05
96	1373.7985	0.05
110	1544.6282	0.08
114	1625.5083	-0.05
126	1753.8693	0.11
128	1776.6010	0.05
129	1784.0095	0.11
130	1785.3942	0.08
131	1827.9013	0.11

Table 1: The vibrational frequency modes on Ex($\mathbf{R}$), having larger absolute value for the scalar product with $\mathbf{F}$.

frequencies are $\hbar\omega_1 = 18$meV (mode 1) and $\hbar\omega_2 = 58$meV (mode 2). The electron-vibration coupling constant for the first mode s_1 is fixed to 1. These values are taken from Ref. [7].

The calculated results of the pump-probe spectra for $s_2 = 0.6$ is shown in Figs. 5-(a) and (b). Although probe response is finite only for discrete values of probe frequencies (Eq. 15), we draw lines which connect spectral lines with finite response, so as to make the overall behavior of spectra clearly shown.

The motion of the excited-state wave packet is understood by tracing the peak of the spectra. However, as shown in Fig. 5-(b), the trajectory of the peak of the spectra corresponds to that for the vibration mode 1, although fine structure due to the mode 2 is also seen in the spectra (see Fig. 5-(a)). In fact, the amplitude of the oscillation in Fig. 5-(b) is ~ 70meV which corresponds to the distance between the two turning points for the mode 1 ($4s_1^2\hbar\omega_1 = 72$meV).

As the value of s_i decreases, the trace of the peak of the spectra is blurred and the turning points become unclear as we mentioned in Section 3.1, and for this reason the turning points corresponding to the mode 2 are not seen in the spectra. As Fig. 5-(a) shows, however, the effect of the mode 2 is clearly seen in the fine structure of the spectra, which means that we understand the wave packet motion corresponding to the mode 2 by accurate measurement of time-resolved spectra. To be more precise, we found that the shape of the spectra is sensitive to the value of s_2 in the present case and that the s_2 is determined by careful observation of the spectral shape. In Figs. 6-(a)-(c) we show the results for $s_2 = 0.5$, 0.6, and 0.7 with the values of the other parameters fixed to those in Fig. 5. The figures show that the shape of the spectra changes rapidly as s_2 is varied. Thus, we can determine the materials parameters regarding with weakly coupled mode by a sort of pattern matching methods for time-resolved spectra, though the precise methods to determine these values have not been well-established. In the case of DTTCI, we found that $s_2 = 0.6$ is most feasible by using Figs. 6-(a)-(c). Hence, the relaxation energy of the excited wave packet is 39meV, which is consistent with the results of molecular orbital calculation shown in Section 3.2.1.

4 Discussion and conclusions

In this paper we calculated the nonlinear optical response of wave packets on quantized potential surfaces. We found that, due to the discreteness of the vibrational eigenstates, the probe signals as a function of pump-probe delay suddenly changes its behavior following the stepwise change of the energy levels of the molecule. This aspect is particularly important when electron-vibration interaction is weak, *i.e.*, the wave packet motion takes place in the vicinity of the bottom of the excited-state PES. In this case, a simple parabolic approximation for PESs is quite good and the analytical formula of the probe signal within impulse approximation is sufficient to discuss experimental results.

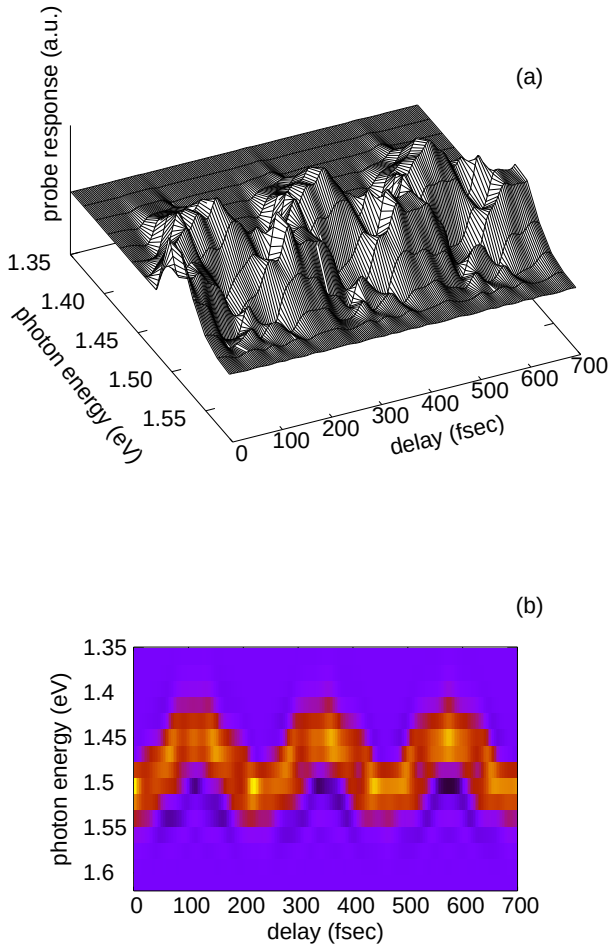

Figure 5: Calculated pump-probe spectra for DTTCI as a function of probe photon energy and the pump-probe delay time: (a) bird's-eye view (b) palette-mapped plot. The values of the parameters are: $\hbar\omega_1 = 18$meV, $\hbar\omega_2 = 58$meV, $\hbar\varepsilon = 1.5$eV, $s_1 = 1$, and $s_2 = 0.6$.

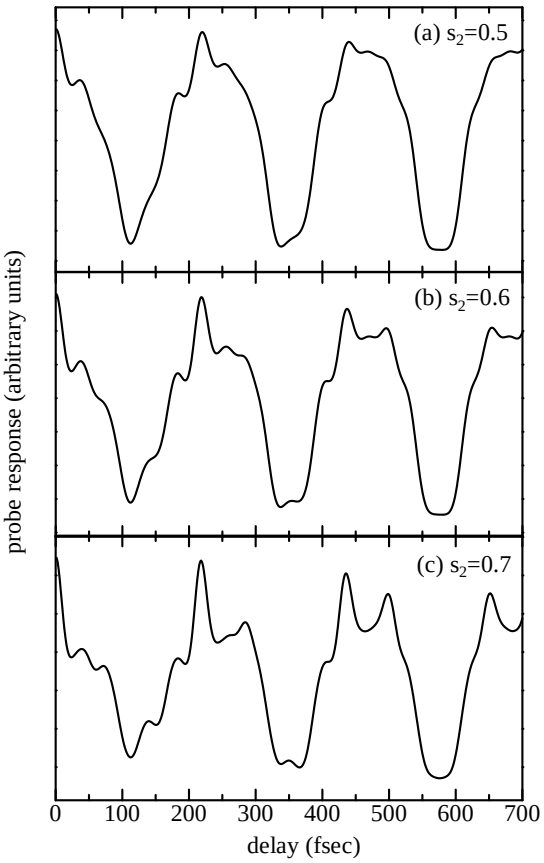

Figure 6: Calculated probe response at $\Omega = 1.52$eV for $\hbar\omega_1 = 18$meV, $\hbar\omega_2 = 58$meV, $s_1 = 1$ and (a)$s_2 = 0.5$, (b)$s_2 = 0.6$, (c)$s_2 = 0.7$.

The calculated results agree well with the pump-probe experimental results on DTTCI, and it is shown that we can estimate the strength of electron-vibration interaction directly from experimental results. These results are also consistent with the molecular orbital calculations. Thus, we stress that the accurate measurement of pump-probe signals combined with theoretical calculations is a powerful tool to understand the wave packet dynamics clearly. Once the dynamics of the wave packets are sufficiently known, we try to design the control method of them, which will bring us, *e.g.*, the efficient way for chemical reaction control, optimization of luminescence intensity from biological samples, or accurate control of qubits stored in various materials such as quantum dots or molecules. We mention that, as a typical example of the control method, the initial condition for the excited wave packet is controlled by pulse chirp[10, 11, 12] and that the probe response is modulated by the presence of chirp. We, however, also note that those results have not reached to control the wave packet motion observing the quantum-mechanical wave packets and hence the design of the control in coherent regime is still on the way even in simple molecular systems.

We should mention that the present calculation does not take into account the effect of decoherence of the vibrational states. Since we are interested in molecules in solution, the relaxation of excited wave packets is important to understand their physical properties even in sub-picosecond regime. These effects necessarily involve the mixed-state description of the wave packets and coarse graining of the dynamical variables consisting of the "environment". It is necessary to obtain various knowledge of the total system (molecules+environment) to develop a quantitative theory of the decoherence in the present system, and thus the problem of decoherence is left for the future. We, however, stress that the present results are still useful as a basis of the study of wave packet dynamics even when the relaxation processes are of importance.

acknowledgements

The authors are grateful to K. Horikoshi for valuable discussions on pump-probe experiments of DTTCI. K. I. also thanks S. Uchikoga and for helpful advice.

A Quantized form and the eigenstates of the Hamiltonian

After canonical quantization of the Hamiltonian (1), it is rewritten as

$$\begin{aligned}\mathcal{H} &= \hbar\sum_{i=1}^{M}\omega_i\left[a_i^\dagger a_i + \{\varepsilon + \frac{s_i^2}{1-t_i} + \frac{1}{2}(1-\sqrt{1-t_i})\right.\\ &+ \left. s_i(a_i^\dagger + a_i) - \frac{t_i}{4}(a_i^\dagger + a_i)^2\}|\uparrow\rangle\langle\uparrow|\right], \end{aligned} \tag{20}$$

where the creation operator of the vibration modes of the ground-state PES is

$$a_j^\dagger = \sqrt{\frac{\omega}{2}} u_i - i \frac{p_j}{\sqrt{2\omega}}. \tag{21}$$

It is diagonalized by introducing unitary transformation

$$U = \prod_{i=1}^{M} U_i, \tag{22}$$

where

$$U_i = \exp\left\{ \frac{\log(1-t_i)}{8} ((a_i^\dagger)^2 - a_i^2) \right\} \exp\left\{ \frac{s_i}{1-t_i} (a_i^\dagger - a_i) \right\}. \tag{23}$$

The eigenvalue and the corresponding eigenvector of the Hamiltonian on the excited-state PES are given by

$$E^\uparrow_{n_1 n_2, \ldots n_M} = \hbar \left(\sum_{i=1}^{M} n_i \sqrt{1-t_i} \omega_i + \varepsilon \right), \tag{24}$$

$$|n_1 n_2, \ldots n_M \uparrow\rangle = \bigotimes_{i=1}^{M} U_i^\dagger |n_i\rangle, \tag{25}$$

and the creation operator of the phonon is

$$b_i^\dagger = a_i^\dagger \cosh\theta_i - a_i \sinh\theta_i - s_i (1-t_i)^{-3/4}, \tag{26}$$

where

$$e^{\theta_i} = (1-t_i)^{-1/4}. \tag{27}$$

When the frequency of the vibrational modes for two PESs is the same, *i.e.*, $t_i = 0$, the above results are identical to those previously obtained[13].

The eigenstates on the excited-state PES for each mode $U_i^\dagger |n_i\rangle$ are expressed by

$$U_i^\dagger |n_i\rangle = \frac{(b_i^\dagger)^{n_i}}{\sqrt{n_i!}} U_i^\dagger |0\rangle = \frac{(a_i^\dagger \cosh\theta_i - a_i \sinh_i \theta_i - s_i (1-t_i)^{-3/4})^{n_i}}{\sqrt{n_i! \cosh\theta_i}} \exp\left\{ \frac{\tanh\theta_i}{2} (a_i^\dagger)^2 \right\} |0\rangle, \tag{28}$$

Thus, the matrix elements of the dipole operator V is given by

$$\langle m_1 m_2 \ldots m_M \downarrow | V | n_1 n_2 \ldots n_M \rangle = \prod_{i=1}^{M} \langle m_i | U_i^\dagger | n_i \rangle, \tag{29}$$

where

$$
\begin{aligned}
\langle m_i|U_i^\dagger|n_i\rangle &= \langle 0|\frac{a_i^{m_i}(b_i^\dagger)^{n_i}}{\sqrt{m_i!n_i!}}U_i^\dagger|0\rangle \\
&= \langle 0|\frac{a_i^{m_i}(a_i^\dagger\cosh\theta_i - a_i\sinh\theta_i - s_i(1-t_i)^{-3/4})^{n_i}}{\sqrt{m_i!n_i!\cosh\theta_i}}\exp\left\{\frac{\tanh\theta_i}{2}(a_i^\dagger)^2\right\}|0\rangle, \\
&= \frac{1}{\sqrt{n_i!m_i!\cosh\theta_i}} \\
&\times \sum_{j=0}^{n_i}\sum_{k=0}^{n_i-j}\sum_{l=0}^{\infty}\frac{(-)^{n_i-j}}{2^l l!}\cosh^{j-l}\theta_i\sinh^{k+l}\theta_1(s_i(1-t_i)^{-3/4})^{n_i-j-k}\langle 0|a_i^{m_i}\{(a_i^\dagger)^j a_i^k\}(a_i^\dagger)^{2l}|0\rangle \\
&= \frac{1}{\sqrt{n_i!m_i!\cosh\theta_i}} \\
&\times \sum_{j=0}^{n_i}\sum_{k=0}^{n_i-j}\frac{(-)^{n_i-j}}{2^{\frac{m_i+k-j}{2}}(\frac{m_i+k-j}{2})!}\cosh^{\frac{3j-m_i+k}{2}}\theta_i\sinh^{\frac{m_i+3k-j}{2}}\theta_i(s_i(1-t_i)^{-3/4})^{n_i-j-k} \\
&\times \langle 0|a_i^{m_i}\{(a_i^\dagger)^j a_i^k\}(a_i^\dagger)^{m_i+k-j}|0\rangle. \qquad (30)
\end{aligned}
$$

$\{(a_i^\dagger)^j a_i^k\}$ denotes the symmetrically ordered product of the operator in the brace[13], and the sum over k is taken only for the integral value of $\frac{m_i+k-j}{2}$.

B probe response by ground-state wave packets

Amongst the third-order polarization terms which appear in the standard perturbation theory[8], the contribution of ground-state wave packets to pump-probe signals is described by, for example,

$$
P_g^{(3)}(t) = \int_0^t\int_0^t\int_0^t dt_1dt_2dt_3E_1(t_1)E_1(t-t_1-t_2)E_2(t-t_1-t_2-t_3)\langle 0\downarrow|VV(t_1)V(t_1+t_2)V(t_1+t_2+t_3)|0\downarrow\rangle, \qquad (31)
$$

where $E_1(t)$ and $E_2(t)$ denote the electric field of the pump and the probe pulse, respectively.

When the pump and the probe pulse are short and they are separated on the temporal axis sufficiently, Eq. (31) for $M=1$ becomes

$$
P_g^{(3)}(t) \sim \bar{S}_1^2\bar{S}_2\sum_{n=0}^{\infty}e^{in\omega T}\langle se^{-i\omega\tau};\uparrow|V|n\downarrow\rangle\langle n\downarrow|Ve^{-\frac{i\mathcal{H}(t-T)}{\hbar}}V|0\downarrow\rangle, \qquad (32)
$$

where $\bar{S}_1$ and $\bar{S}_2$ are the pulse area of the pump and the probe pulses, respectively. τ and T denote the duration of the pump pulse and the pump-probe delay. Since $\langle 0\downarrow|Ve^{-\frac{i\mathcal{H}(t-T)}{\hbar}}V|0\downarrow\rangle$

corresponds to the ground state absorption which is independent of T, the vibronic ground state $|0\downarrow\rangle$ in Eq. (32) does not contribute to the T-dependent part of $P_g^{(3)}(t)$, and is irrelevant to the oscillatory behavior of the time-resolved spectra. Hence, the magnitude of the temporal oscillation in time-resolved spectra given by the ground-state wave packets is estimated by the factor $|\langle se^{-i\omega\tau};\uparrow|V|n\downarrow\rangle|^2$ which is interpreted as the transition probability of vertical transition between excited-state wave packets and ground-state wave packets.

It is quite easy to extend the above discussion to multi-dimensional cases ($M \neq 1$), and we obtain the generalized formula to estimate the effect of ground-state wave packets as

$$\begin{aligned} r^j_{n_1 n_2 \ldots n_M} &= |\langle n_1 n_2 \ldots n_M \downarrow |V| s_1 e^{-i\omega_1\tau} s_2 e^{-i\omega_2\tau} \ldots s_M e^{-i\omega_M\tau};\uparrow\rangle|^2 \\ &= \prod_{j=1}^{M} \exp\{-2s_j^2(1-\cos\omega_j\tau)\}\frac{\{2s_j^2(1-\cos\omega_j\tau)\}_j^n}{n_j!}. \end{aligned} \tag{33}$$

References

[1] For a review, see, "Optical Control of Molecular Dynamics" by S. A. Rice and M. Zhao, (Wiley, New York, 2000).

[2] M. Dantus, M. J. Rosker, and A. H. Zewail, J. Chem. Phys. **87**, 2395 (1987).

[3] H. L. Fragnito, J. Y. Bigot, P. C. Becker, and C. V. Shank, Chem. Phys. Lett. **160**, 101 (1989).

[4] C. J. Bardeen, Q. Wang, and C. V. Shank, Phys. Rev. Lett. **75**, 3410 (1995).

[5] W. T. Pollard, S. L. Dexheimer, Q. Wang, L. A. Peteanu, C. V. Shank, and R. A. Mathies, J. Phys. Chem. **96**, 6147 (1992).

[6] A. T. N. Kumar, F. Rosca, A. Widom, and P. M. Champion, J. Chem. Phys. **114**, 6795 (2001).

[7] K. Horikoshi, K. Misawa, R. Lang, and K. Ishida, Opt. Commun. **259**, 723 (2006).

[8] S. Mukamel, "Principles of Nonlinear Optical Spectroscopy", (Oxford University Press, New York, 1995).

[9] Gaussian 98, Revision A.10, M. J. Frisch, G. W. Trucks, H. B. Schlegel, G. E. Scuseria, M. A. Robb, J. R. Cheeseman, V. G. Zakrzewski, J. A. Montgomery, Jr., R. E. Stratmann, J. C. Burant, S. Dapprich, J. M. Millam, A. D. Daniels, K. N. Kudin, M. C. Strain, O. Farkas, J. Tomasi, V. Barone, M. Cossi, R. Cammi, B. Mennucci, C. Pomelli, C. Adamo,

S. Clifford, J. Ochterski, G. A. Petersson, P. Y. Ayala, Q. Cui, K. Morokuma, P. Salvador, J. J. Dannenberg, D. K. Malick, A. D. Rabuck, K. Raghavachari, J. B. Foresman, J. Cioslowski, J. V. Ortiz, A. G. Baboul, B. B. Stefanov, G. Liu, A. Liashenko, P. Piskorz, I. Komaromi, R. Gomperts, R. L. Martin, D. J. Fox, T. Keith, M. A. Al-Laham, C. Y. Peng, A. Nanayakkara, M. Challacombe, P. M. W. Gill, B. Johnson, W. Chen, M. W. Wong, J. L. Andres, C. Gonzalez, M. Head-Gordon, E. S. Replogle, and J. A. Pople, Gaussian, Inc., Pittsburgh PA, 2001.

[10] C. J. Bardeen, Q. Wang, and C. V. Shank, J. Phys. Chem. **A102**, 2759 (1998).

[11] K. Misawa and T. Kobayashi, J. Chem. Phys. **113**, 7546 (2000).

[12] S. Malkmus, R. Dürr, C. Sobotta, H. Pulvermacher, W. Zinth, and M. Braun, J. Phys. Chem. **A109**, 10488 (2005).

[13] K. E. Cahill and R. J. Glauber, Phys. Rev. **177**, 1857 (1969).